Energized IOT Sensor through RF Harvesting Energy

https://doi.org/10.3991/ijoe.v18i09.30839

Mohamed Zied Chaari[1](✉), Rashid Al-Rahimi[1], Otman Aghzout[2]
[1]FABLAB Department Doha, Qatar Scientific Club, Doha, Qatar
[2]Department of Computer Science and Engineering, SIGL-Lab ENSA, Tétouan, Morocco
chaari_zied@ieee.org

Abstract—Wireless Power Collecting (WPC) present the future in powering and energizing intelligent Internet of Things (IoT) electronics devices. This paper studies and utilizes a circuit to powering wirelessly IoT devices. The WPC offer a best technique to help researchers and engineers of modern societies to build cell blocks. The concept is to energy any IoT devices and sensors wirelessly from Radio Frequency (RF) power strength in the same areas that may be hard to achieve or potentially hazardous. We implemented the RF harvesting technology with IoT devices to increase the efficiency of sensors. The idea of this system is to power up and self-energize any IoT sensors wirelessly. This work studies two different topologies of a rectangular patch antenna and different RF harvesting circuit voltage multiplier configurations using a microwave power station as the input RF source. This work aims to utilize the wireless power transmission technique in the smart house solution. The proposed prototype gets all technical parameters to generate enough electricity to power up the bulbs 5 W wirelessly at a gap distance around a five meters. Finally, we test the RF rectifier circuit coupled with a twin patch antenna that can self-energize the bulb, eventually devices work without batteries.

Keywords—rectenna, wireless power harvesting, patch antenna, Radio Frequency, IoT sensors

1 Introduction

Harvesting energy, usually known as wireless power transmission, is a favorable technique that provides electricity in inaccessible areas [1]–[4]. It is also known as radiofrequency harvesting. Its capability to power up wirelessly electronics devices with low power consumption current. Research in this field recently gathered a lot of attention due to the potential of charging sensors wirelessly in problematic places and areas, investigating wireless power charging by using RF harvesting energy [5]. The essential theory behind this technique is to harvest the RF energy around the antenna or receiver to power sensors. Therefore, the IoT sensors need to have battery-less power supply systems. We will need more recourses to maintain IoT devices in the future because wireless sensor networks usually have many sensors, and, therefore, individual sensors must be without batteries to make them require no maintenance. Wireless power transfer or RF harvesting energy is a favorable technique because it

can energize any IoT devices in a longer energy transfer distance than other competing solutions [6], as shown in Figure 1. Many prominent researchers have contributed to RF energy harvesting with different methods and techniques [7], [8]. Chang-Yeob Chu et al. studied a system design for electric automobile charging considering a wide range of coupling coefficient variation depending on coil misalignment [9]. Koichiro Ishibashi et al. suggested the RF characteristics of rectifier devices for ambient RF energy harvesting [10]. Rashid Al Rahimi et al. investigated the impact of wireless energy transmission on the future of the battlefield in many places worldwide and the effect of this technology ranking of countries in terms of military power [11]. The investigation considered two levels the impact of the RF power sources and the effect of the distance in the attenuation. Mohamed Zied et al. developed energized IoT sensors through RF energy recovery [12]. According to Mohamed Zied et al.'s analysis, all technical factors offer adequate electricity to energize bulb 5 W wireless at a distance gap arround five meters [13]. Nermeen A. Eltresy et al. studied a CPIFA antenna to collect the RF energy at three different frequency bands of GSM 900, GSM 1800, and Wi-Fi 2400 [14]. According to their analysis, the aim of designing a matching circuit is to match the proposed antenna with a rectifier to get maximum power transfer and minimum loss. They successfully harvested an output of 624 mV at 0 dBm input power [8]. Diffa Pinto et al. evaluated the performance and established a relationship between process parameters to harvest energy and the number of the rectifier circuit.

They created a circuit for a Wi-Fi power-gathering system using the seven-stage Villard voltage booster circuit, designed and evaluated using Agilent Design Systems (ADS) software [15]. The power management unit receives the output voltage of the Villard rectifier circuit. According to their analysis, the final simulated output voltage of 12V is achieved. With the growth applications related to IoT devices, smart home communication, environmental monitoring, and intelligent healthcare [16]–[19].

The major objective of the work is as follows:

- To develop a battery-free wireless power source from an available RF station fixed in the roof of the house,
- To create a twin pin feed patch antenna with high Gain and directivity,
- To create a power conversion circuit with high efficiency to extract enough electricity,

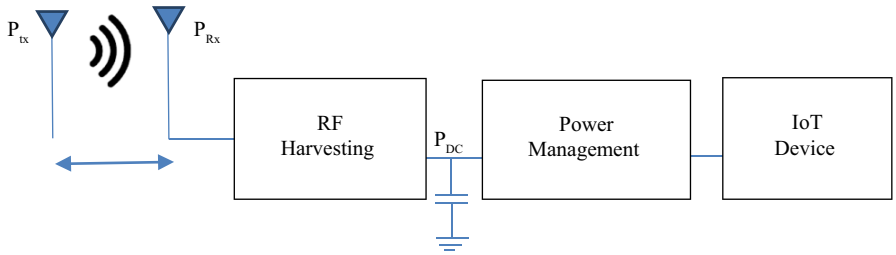

Fig. 1. Typical block diagram to energize IoT sensor wirelessly

This study can harvest RF energy from a radio frequency source. The frequency of the RF power source is 2.45 GHz, and output power is around 20W. With this study,

we can provide the two most critical elements for the IoT device fixed on the smart house the electricity to energize the battery of any electronic device and keep the all-time battery self-powered by RF radiation. This study concentrates on the opportunity of activating electronic devices from the RF harvester device already mounted and repaired within the IoT devices. This study shows the utility of using wireless power harvesting in the intelligent house, making our lives more intelligent and safer. The receiver RF energy is then made efficient via the rectifier circuit utilizing Schottky diodes, connected directly to the LED bulb, as shown in Figure 2.

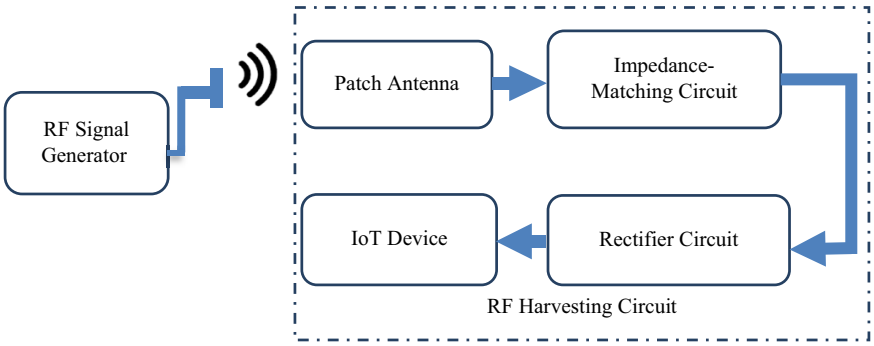

Fig. 2. Block diagram showing energized IoT devices through RF wireless power transfer

The topology design contains three main subsystems, each having specific purposes. The RF emitter station is with low power and high frequency. The microstrip antenna captures electromagnetic radiation from the microwave power station. The DC storage device accumulates DC power from the rectifier circuit. The following subsection will examine and analyze the rectifier topologies. This chapter focuses on the patch antenna and device characteristics of RF energy-harvesting systems. RF characteristics of the electronics parameters of the Schottky diode, which are suitable for efficiently rectifying the RF signal, are shown. The experiments for RF energy scavenging from ambient RF signals use multiple topologies: single-stage voltage double, bridge rectifier circuit, and the five-stage Villard rectifier voltage circuit to exhibit more than 5W power generations.

This research is planned as follows: Section 1 is the introduction. Then in Section 2, we study the antenna fabrication, experimental measurements, and simulation Techniques. In Section 3, we present the power budget. In Section 4, we discuss the rectifier investigation and results. Finally, we finalize a prototype device discussion and conclude the future work.

2 Antenna fabrication, simulation techniques, and experimental measurements

Most challenges come from implementing the harvesting circuit inside the IoT device, and it is essential to reduce the size of the RF scavenging circuit. The patch

antenna is a suitable antenna meeting these obligations due to its flexibility of possible geometry and pure integrity with any IoT device [20]. Depending on the antenna beam-width, the radiation power ratio will differ. We study two different configurations of a rectangular patch antenna: one without inset feed and another with inset feed.

2.1 Twin without inset-fed patch antenna

The patch antenna size is generally depending on the resonant frequency (f_r) and the substrate dielectric ε_r, where the width (W_p) of the antenna is calculated using Equation (1):

$$W = \frac{c}{2 \times fr \times \sqrt{\frac{\varepsilon + 1}{2}}} \tag{1}$$

The patch antenna length (L_p) can be calculated as follows in Equation (2):

$$L_P = \frac{C}{2 \times fr \times \sqrt{\varepsilon_{reff}}} \tag{2}$$

For calculating the input impedance Z_0, we use Equation (3):

$$Z_0 = R_{in} \times cos^2 \times \left(\frac{\pi}{Lp} - d \right) \tag{3}$$

where
C: The speed of light,
ε: The effective dielectric, and
d: The depth of the inset feed,
Equation (4) is used to calculate the length of the ground plane:

$$L_g = L + 6h \tag{4}$$

Based on Equation (5), we can calculate the width of the antenna ground plane (Wg) as follows:

$$W_g = W + 6h \tag{5}$$

The optimized parameters of the patch antenna are present in Table 1:

Table 1. Optimal patch antenna parameters

Operating frequency	2.45 GHz
Dielectric constant	4.6
Substrate thickness	1.6 mm
The thickness of the copper	35 µm
Tang (d)	0.01
Copper conductivity	5.8 e^7 S/m
Ground conductor Thickness	35 µm
R_{in}	50Ω

We aimed to use the RF4 substrate. The substrate's thickness will influence the performance of the patch antenna [21]. In most cases, the wavelength should not be smaller than 0.05 mm. Therefore, we might as well set it to 1.6 mm, as illustrated in Figure 3:

Fig. 3. RF4 substrate properties window

Antennas have been simulated using the Advanced Design System (ADS). ADS is an electronic design automation system produced by Agilent EEsof EDA, a division of Agilent Technologies. It offers combined design tools for designers of RF electronic products such as mobile phones, antennas, patch antennas, satellite signals, RF modulation, and RF jammers. Figure 4a shows the schematic of the microstrip patch antenna with the optimal parameters for microstrip line (MLIN), microstrip line open-circuited stub (MLOC), microstrip curve (MCURVE), and microstrip coupled line (MSTEP). The patch antenna isometric layout is shown in Figure 4b.

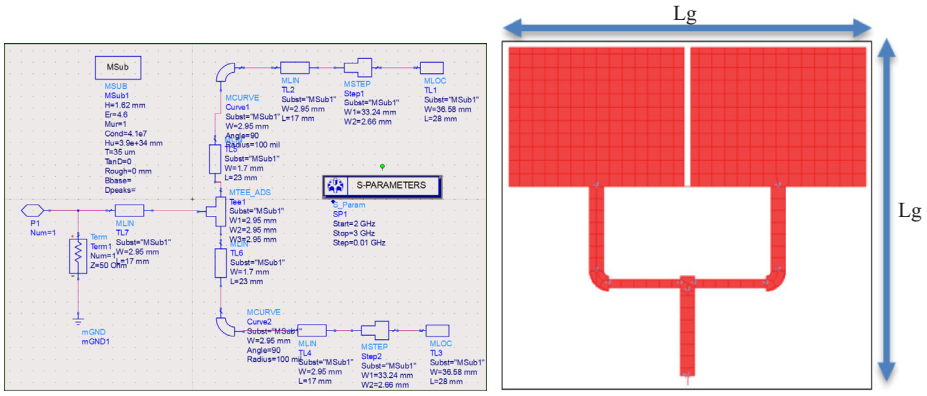

Fig. 4. (a) Microstrip patch antenna design in the schematic, (b) Isometric layout

This subsection analyzes the physical performance parameters of this antenna. The simulations were run using ADS software, a high-frequency simulation tool. In the Figures below, we can see the results of the simulations. Figure 5 displays the twin patch antenna built.

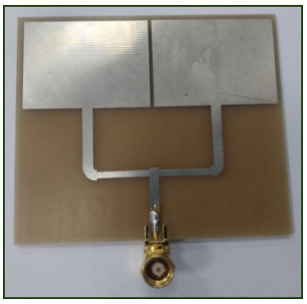

Fig. 5. Build the twin patch antenna

Directivity. As shown in Figure 6, the directivity of the proposal patch antenna showing at 2.444 GHz is 7.339 dBi, and the Gain is equal to 5.282 dBi.

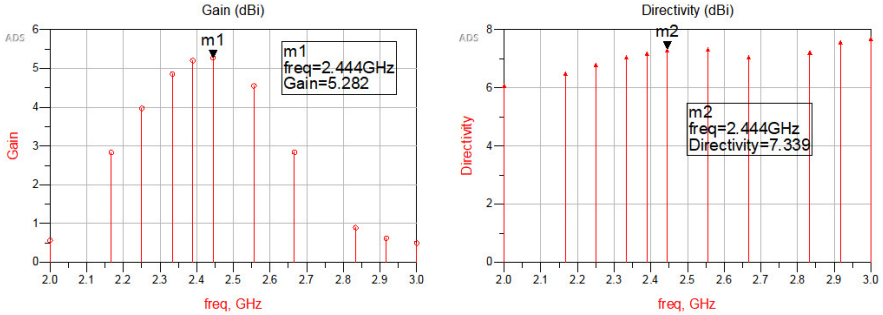

Fig. 6. Gain and directivity of the twin patch antenna

Reflection coefficient of the antenna. As illustrated in Figure 7, we obtained a satisfactory return loss of S11 = –8.921dB. The antenna has a bandwidth of 29 MHz and a standing wave ratio of 1.056 at 2.45 GHz.

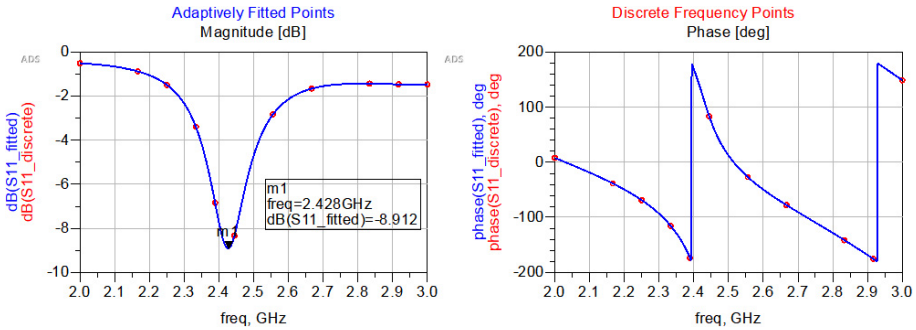

Fig. 7. Antenna S11 performance

Radiation pattern 3D. Based on a 3D radiation pattern, the proposed antenna has 7.22 dB of directivity, as shown in Figure 8:

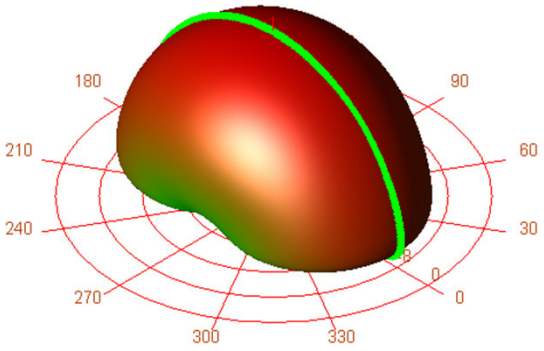

Fig. 8. The proposed antenna radiation pattern in 3D

Current distribution. Simulation results showed that the current distributions were different for different frequencies. Figure 9 shows a high amount of current at 2.45 GHz.

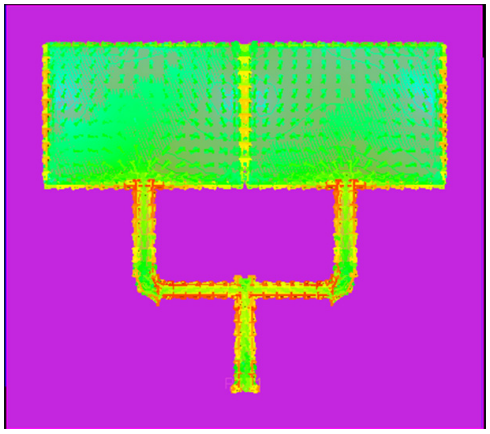

Fig. 9. Distribution of antenna currents

Smith plot. On frequency 2.448 GHz, we can see that the twin antenna perfectly matched the input RF signal, with a low imaginary part for the impedance. Therefore, all signals at the operating frequency are transmitted, as shown in Figure 10.

Where:

$$Z = (Z_0 \times (0.850 - j0.063)). \quad (6)$$

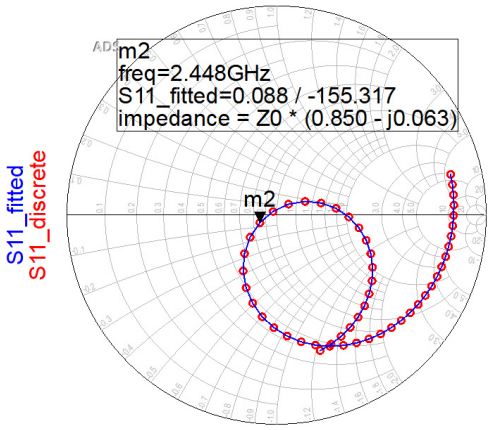

Fig. 10. Antenna Smith chart

The performance of this antenna is acceptable for harvesting RF energy. In the following stage, we try to upgrade the performance of this antenna by adding an inset feed and seeing the results.

2.2 Twin inset-feed patch antenna

A schematic for the patch antenna is provided below, representing the optimum parameters for Microstrip Line (MLIN), Microstrip Line Open-Circuited Stub (MLOC), and Microstrip Asymmetric Coupled Line (MACLIN). As shown in Figure 11, the feed line is inset by using a MACLIN. According to Equation (7), W1, and W3, are equal and calculated based on the substrate's width:

$$W1 = W3 = \frac{W-9}{2} \tag{7}$$

The width (W) of the antenna microstrip line feed, as shown in Equation (8), is equivalent to W2.

Also, S1 and S2 are the gaps of the inset feed, where both were equal to W_f.

The width of the microstrip line feed, W_f, can be calculated using Equation (8):

$$W_f = \{(\frac{e^H}{8} - \frac{1}{4e^H})^{-1}\} \times 1.6mm \tag{8}$$

In addition, the microstrip line feed length, W_f, can be calculated from Equation (9) below:

$$L_f = \theta \frac{\lambda_g}{360^0} \tag{9}$$

where (λ_g):

$$\lambda_g = \frac{C}{f \times \sqrt{\varepsilon_{reff}}} \tag{10}$$

For calculating notch width, we use Equation (11):

$$g = \frac{c \times 4.65 \times 10^{-12}}{\sqrt{2 \times \varepsilon} \times f_r} \tag{11}$$

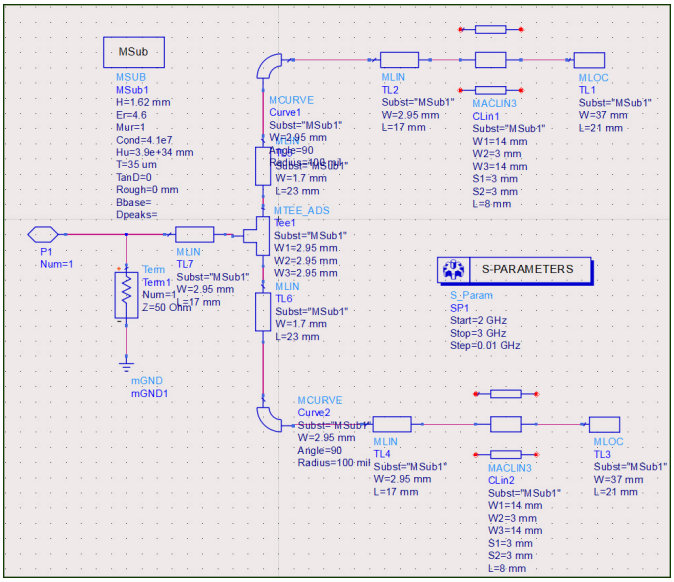

Fig. 11. Optimized circuit schematics of twin inset-feed patch antenna

With the FR4 dielectric substrate (= 4.6, tanδ = 0.02, and h = 1.6mm), f = 2.4 GHz, the relative bandwidth is more than 1%. Based on the above formulas, the length and width (L = 3.7cm, W = 2.1cm) can be determined. A simulation of the twin patch antenna is shown in the next subsection.

Directivity. As shown in Figure 12, the proposed twin inset-feed patch antenna has a directivity of 7.33 dBi and a gain of approximately 3.681 dBi.

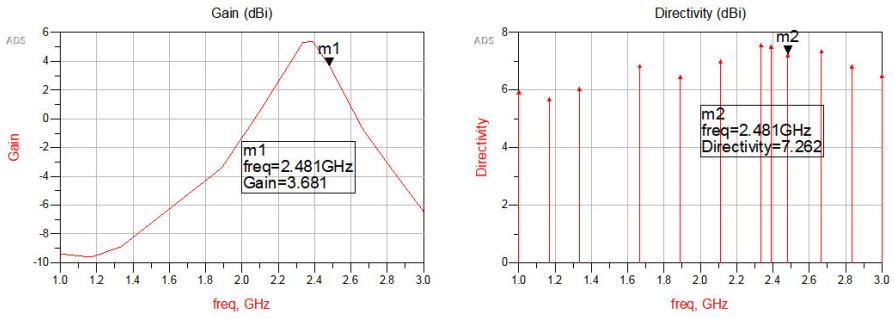

Fig. 12. Gain and directivity of the twin inset-feed patch antenna

Reflection coefficient of the antenna. Based on Figure 13, we obtained a reasonable return loss value of –28.610 dB at 2.422 GHz. As a result, the antenna at 2.422 GHz has a standing wave ratio of 1.056 and a bandwidth of 31 MHz.

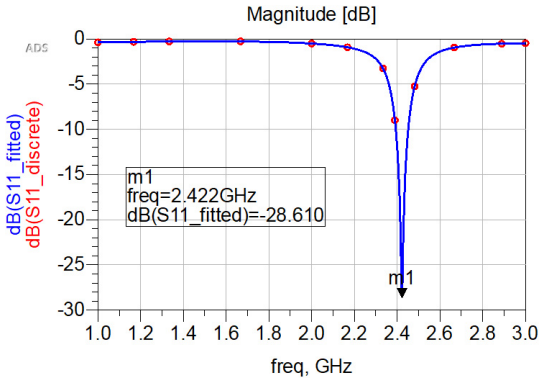

Fig. 13. S11 of the twin inset-feed patch antenna

Radiation pattern 3D. The radiation pattern of the twin inset-feed patch antenna shows how much energy it radiates. Radiation patterns include 3D radiation patterns, 2D radiation patterns, and lobe formation radiation patterns. Figure 14 illustrates the elevation pattern of the antenna in a 3D radiation pattern.

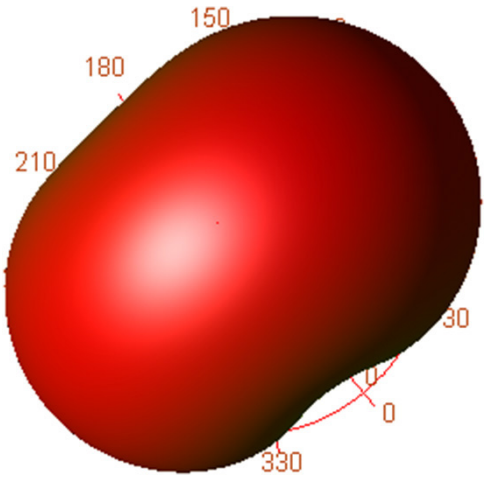

Fig. 14. The radiation pattern of the proposed twin inset-feed patch antenna in 3D

Current distribution. According to the simulation, the current distributions differed for different frequencies. As can be seen in Figure 15, we had a high current distribution at 2.45 GHz:

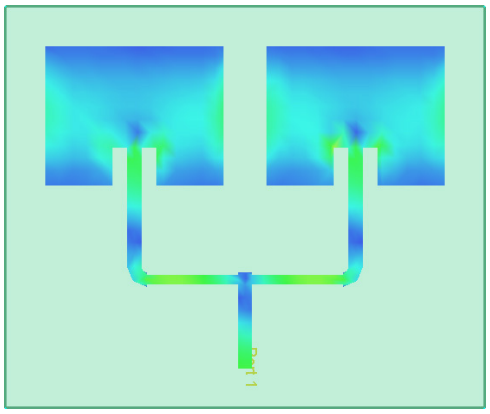

Fig. 15. Current antenna distribution

Smith plot. At 2.422 GHz, the antenna almost perfectly matches the signal source with no imaginary impedance part. Therefore, all signals at 2.422 GHz will be transmitted, as shown in Figure 16.

Where

$$Z = (Z_0 \times (0.938 + j0.037))$$

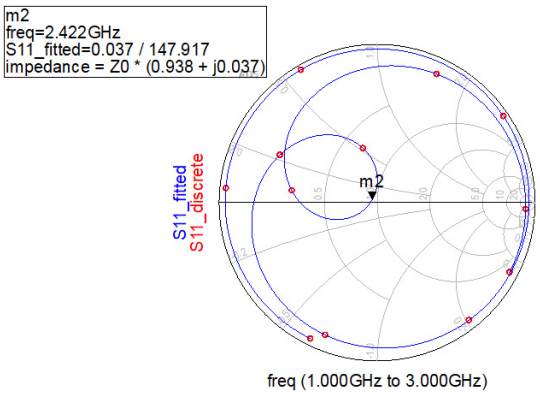

Fig. 16. Plot of the Smith chart for the proposed antenna

Table 2 compares the twin patch antenna without inset feed with the twin patch antenna with inset feed and the same substrate parameters. Based on the comparison of the designed antennas, we can determine the most influential parameters that affect the antenna.

Table 2. Comparison of the two antennas

Antenna	Input Power (mW)	S11 (dBi)	Directivity (dBi)	Gain (dBi)	Radiation Efficiency (%)	VSWR
Twin patch antenna without inset feed	209	–8.912	7.44	5.25	60.30	1.123
Twin inset-feed patch antenna	175.5	–28.61	7.27	3.844	45.438	1.078

The results show that the antenna bandwidth is smaller after inserting the single slot in a twin inset-feed rectangular microstrip patch. Because of the slotting technique, the proposed antenna design has a bandwidth of 0.670 GHz. We selected an inset-feed patch antenna with FR4 dielectric substrate based on the results in Table 2.

3 Power budget

The following part introduces the effective areas of the receiving and transmitting antennas and calculates the required transmitter power for various ranges as shown in Figure 17:

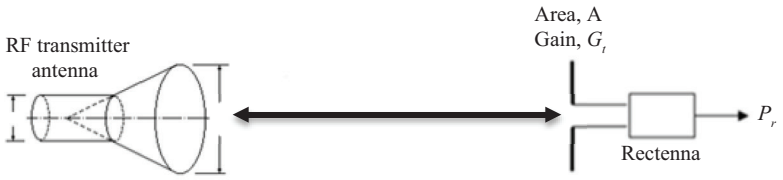

Fig. 17. Antenna and rectenna diagram

Over a perfect ground plane, the patch antenna's effective area is calculated as follows:

$$A_{er} = \frac{G_r \lambda^2}{4\pi} \tag{12}$$

where the wavelength

$$\lambda = \frac{C}{f} = \frac{3.10^8}{2.45.10^9} = 0.122m = 12cm,$$

G_r is the antenna's Gain, and λ is the wavelength at 2450 MHz. From Table 2, the Gain is G = 5.25 dBi. Based on Equation (12), the effective area of the dipole antenna is $6.22 \times 10^{-3} m^2$. The power density Wi of the conical horn antenna at distance R can be expressed as follows:

$$W_i = \frac{P_t G_r}{4\pi R^2} = \frac{P_t A_{et}}{\lambda^2 R^2} \tag{13}$$

Where

P_t Power transmitted,

A_{et} The effective area of the conical antenna,

R: The distance between the transmitting antenna and the patch antenna.

The Gain of a conical horn antenna can be expressed as follows:

$$G = \left(\frac{\pi D_f}{\lambda}\right)^2 A_{er}.$$

The aperture efficiency e_A can be expressed as

$$A_{er} = \frac{G}{\left(\frac{\pi Df}{\lambda}\right)^2} = \frac{7.22}{\left(\frac{3.14 \times 0.27}{0.122}\right)^2} = 0.1495 m^2.$$

Conical horn antennas have an effective area equal to the physical area (A) times the efficiency. Based on the assumption that the conical horn diameter Df = 270.2 mm, the power received by the dipole antenna is given by

$$P_r = W_i A_{er} = \frac{P_t A_{et} A_{er}}{\lambda^2 R^2} \tag{14}$$

To achieve 5W at the receiver, Equation (14) shows the power required to transmit versus the distance between the receiving and transmitting antennas. According to this analysis, R is within the far-field of the conical horn antenna. The sketch of the conical horn antenna appears in Figure 18.

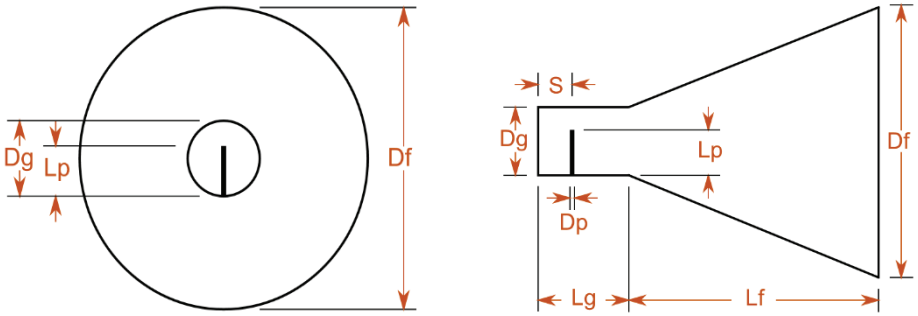

Fig. 18. Conical horn antenna sketch: (a) End view, (b) Side view

Table 3 presents the conical horn antenna physical parameters:

Table 3. Conical horn antenna physical parameters

Name	Description	Value
Dg	Diameter of the waveguide	82.72 mm
Lg	Waveguide length	183.5 mm
Df	Flare diameter	270.2 mm
Lf	Length of the flare	113.2 mm
Lp	Length of the feed pin	27.53 mm
S	Feed-pin inset (distance from back-wall)	43.44 mm
Dp	Feed pin diameter	1.224 mm

The next step is to evaluate the performance of various rectenna configurations by simulating the conversion efficiency and analyzing the Schottky diode model parameters to analyze the effect of changing the design.

4 Rectifier investigation

This section will study the construction of RF rectifiers; we will select the components according to the output voltage and output current. Analyze the response of the RF rectifier circuit depending on the diode parameters, as shown in Figure 19. The output voltage (Vout) obtained is a function of (RL) value, as shown in Equation (15):

$$V_{out} = V0\left(\frac{1}{\frac{R_0}{R_L}+\frac{1}{n}}\right) \tag{15}$$

According to Table 4, several research studies have recently advanced the development of voltage multipliers for wirelessly powering IoT devices.

Table 4. The latest developments in the voltage multiplier field

Ref	Frequency Range	Number of Stages	Comments
Hong et al., 2013	2.48 GHz	Seven stages	This work presents that can harvest voltage around 2.3V.
Akter et al., 2014 [22]	0.9 GHz	Five stages	This work presents that can harvest V_{out} = 2.5V I_{out} = 25µA
Esraa et al., 2015 [23]	0.9 GHz	Three stages	This circuit is improved and reached by using HSMS 285B Schottky diode.
Rashid et al., 2017 [24]	2.45 GHz	Four stages	This rectifier outputs 5.25 volts.

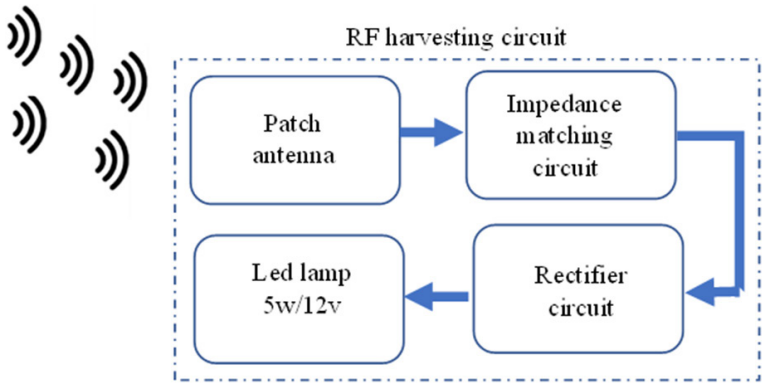

Fig. 19. RF harvesting circuit block diagram

4.1 Single-stage voltage double RF energy harvesting circuit

The harvested DC power function is validated using Equation (15) through circuit simulation on ADS. We use the Schottky diode HSMS2860 because it operates at a shallow input RF power level, as shown in Figure 20.

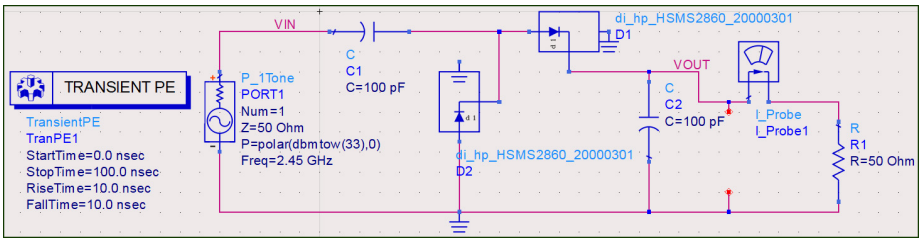

Fig. 20. Single-stage voltage double RF energy harvesting circuit

In the simulation of the rectification subsystem, diode HSMS2860 uses. The following simulation shows the output voltage (Vout) and the output current (Iout) from the single-stage voltage double RF energy harvesting circuit, as shown in Figure 21. The DC-biased HSMS-286x recommend at higher frequencies. The HSMS-286x series is a high-performance diode with low capacitance and superior forward voltage.

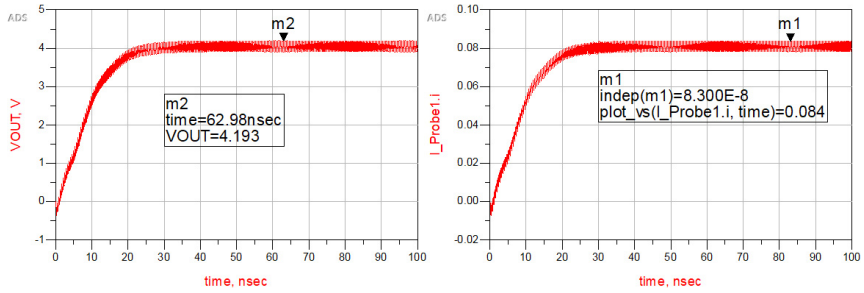

Fig. 21. The rectifier circuit's simulated output voltage (V_{out}) and current (I_{out})

In the absence of a capacitor, the output signal is not excellent, but there is an extra offset AC signal. Input microwave signals are charged up to the peak value of the capacitors, and they are discharged to the Schottky diode's resistance (RL). Due to this, the Vout through the capacitor is almost four times the Vin. Ultimately, the measurement reveals that Vout is simply the multiplication of Vin.

The harvesting power (W) is affected by the RF diode parameters. Six RF diodes with different parameters were used to simulate the same circuit. Table 5 presents the conversion efficiency in relation to the diode parameters, which can be used to estimate the effect of each diode parameter on the RF rectifier:

Table 5. Efficiency comparison among Schottky diode HSMS-2800, HSMS-2850, HSMS-2860, HSMS-2810, HSMS8101, HSMS2700, and HSMS-270B

Diode	P_{in} (dB)	Load Resistance (Ω)	V_{out} (v)	I_{out} (mA)	P_{out} (w)	Efficiency $\eta = \frac{V_{out} \times I_{out}}{P_{in}}(\%)$
HSMS2800	33	50	4.48	90	0.4	12.21
HSMS2850			1.70	34	0.058	1.75
HSMS2860			4.19	84	0.35	10.67
HSMS2810			6.58	132	0.86	26.33
HSMS8101			4.21	84	0.354	10.72
HSMS2700			3.74	75	0.28	8.51
HSMS270B			3.63	73	0.264	8.03

The SPICE parameters on each datasheet make it easy to compare the characteristics of each diode series in the HSMS diode family. This explains how the RF rectifier efficiency varies considerably.

4.2 RF harvesting circuit design uses a bridge rectifier

The proposed harvesting circuit uses a bridge rectifier circuit to generate enough DC voltage from low incident RF power. RF energy harvesting circuits can be designed using this rectifier topology. The circuit design for the rectenna subsystem using RF diode HSMS8101 is shown in Figure 22:

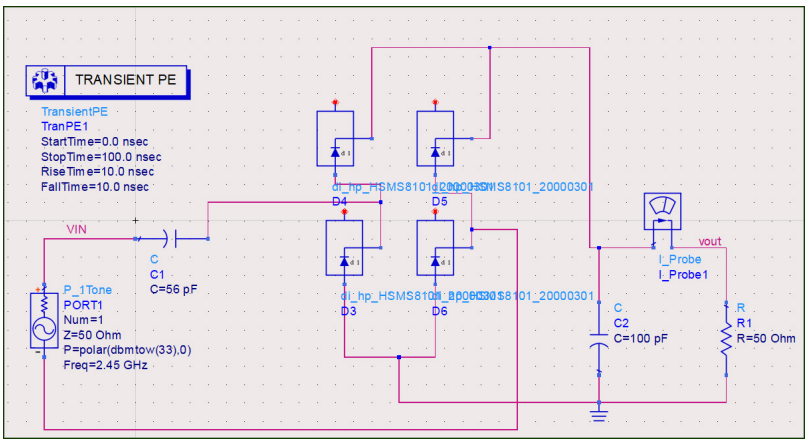

Fig. 22. The circuit design of the rectenna (Agilent ADS)

In Figure 23, the output voltage (Vout = 4.722) and current (Iout = 94mA) are shown:

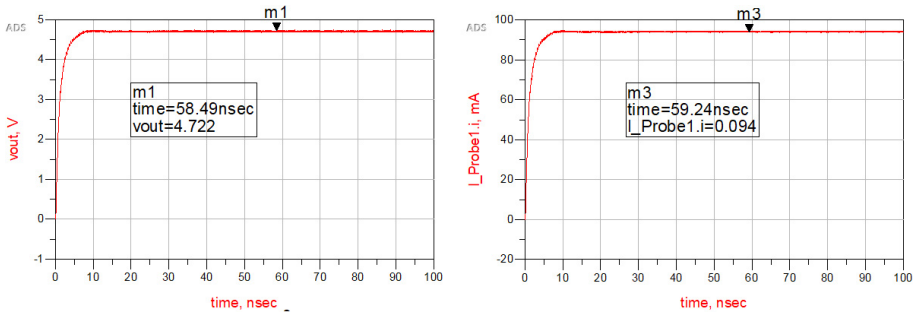

Fig. 23. The rectifier circuit's simulated output voltage (V) and the output current (I)

In the power conversion circuit, diodes play a crucial role. Table 6 illustrates how to bridge rectifier efficiency varies with diode parameters for RF harvesting circuit design. The HSMS diode should have a low recovery time to achieve high conversion efficiency. The Schottky diode HSMS2810 was selected as the best conversion device to design the rectifier. According to this equivalent circuit, series resistance RS = 15Ω, zero bias junction capacitor Cj0 = 1.2 pF, maximum forward voltage VF = 410 mV, and minimum breakdown voltage VB = 20V.

Table 6. HSMS-2800, HSMS-2850, HSMS-2860, HSMS-2810, HSMS8101, HSMS2700, and HSMS-270B: Comparison of efficiency

Diode	P_{in} (dB)	Load Resistance (Ω)	V_{out} (v)	I_{out} (mA)	P_{out} (w)	Efficiency $\eta = \frac{V_{out} \times I_{out}}{P_{in}}(\%)$
HSMS2800	33	50	4.96	98	0.48	14.72
HSMS2850			2.11	42	0.08	2.68
HSMS2860			4.66	93	0.43	14.44
HSMS2810			7.072	140	0.99	30.00
HSMS8101			4.722	94	0.44	13.45
HSMS2700			4.913	98	0.43	14.59
HSMS270B			4.32	86	0.36	11.25

4.3 RF harvesting circuit design uses a five-stage voltage multiplier

As shown in Figure 24, the five stages voltage multiplier consists of the Schottky diode HSMS2820 for harvesting RF energy. Higher Vout could be obtained by increasing the number of steps, and lower Vout was obtained by reducing the number of steps.

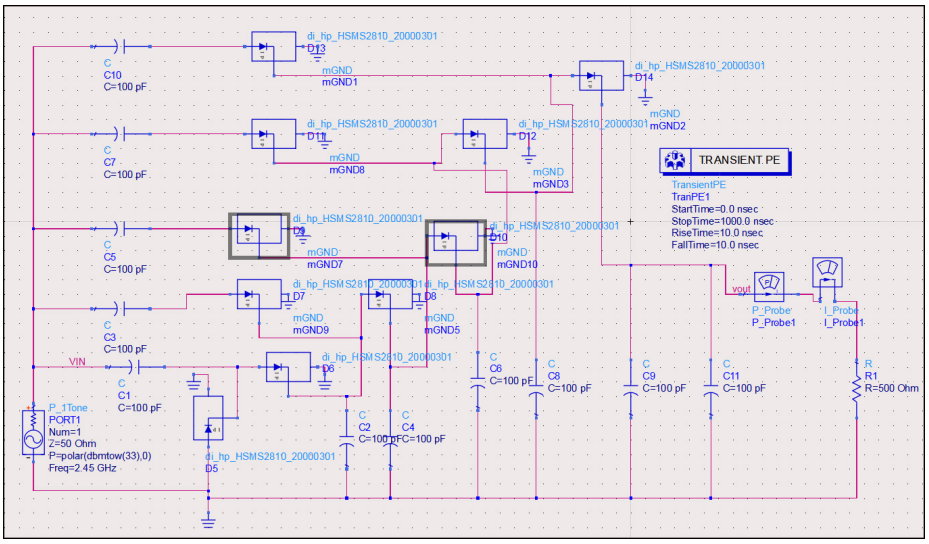

Fig. 24. Design of RF harvesting circuits using five-stage voltage multipliers with diode HSMS-28XX

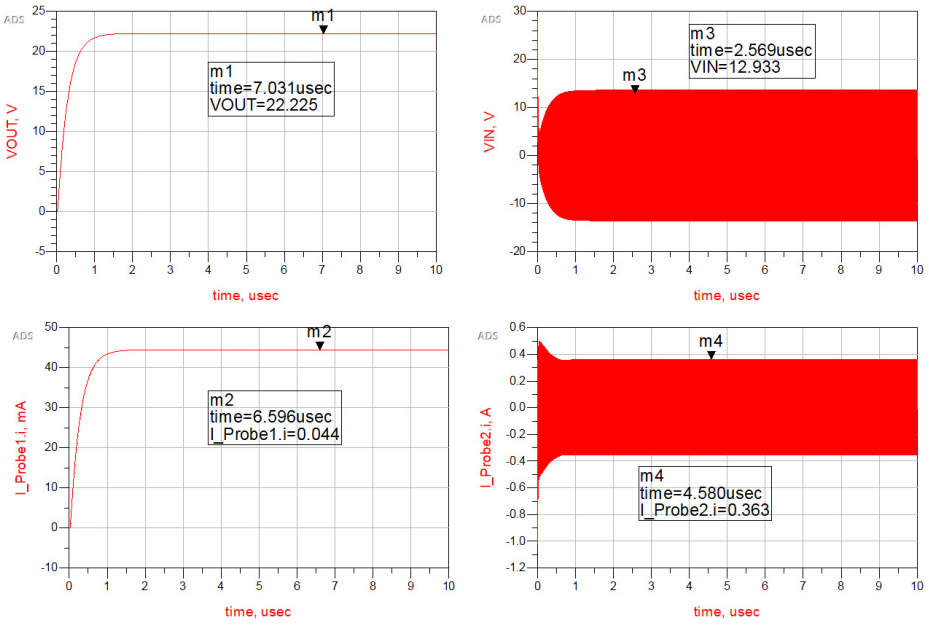

Fig. 25. Optimized simulation results

As seen in Figure 25, this result shows the DC output voltages through a simulated five-stage voltage multiplier of 7.18 V at 30 dBm, with rectifier Schottky diode HSMS2700.

Table 7. Schottky diode HSMS-2800, HSMS-2850, HSMS-2860, HSMS-2810, HSMS8101, HSMS2700, and HSMS-270B efficiency comparison

Diode	P_{in} (dB)	Load resistance (Ω)	V_{out} (v)	I_{out} (mA)	P_{out} (w)	Efficiency $\eta = \frac{V_{out} \times I_{out}}{P_{in}}(\%)$
HSMS2800	33	500 Ω	9.75	20	0.19	5.91
HSMS2850			2.00	4.12	0.0081	0.25
HSMS2860			3.86	8	0.03	0.93
HSMS2810			11.60	23	0.27	8.09
HSMS8101			6.64	13	0.088	2.61
HSMS2700			7.18	14.2	0.103	3.09
HSMS270B			0.24	0.52	$1.06e^{-4}$	0.003

The HSMS-28xx family uses the same diode package, but the chip configurations differ. HSMS-281x diodes produce low-level flicker noise. Due to their excellent RF characteristics, the low forward voltage at high current levels, and low input resistance, the HSMS-282x series diodes are considered among the most appropriate diodes for microwave harvesting. This diode is a family of zero-bias detectors for small signal (Pin = 33 dB) applications below 1.5 GHz, as shown in Table 7. HSMS-285x diodes are suitable for large-RF signal purposes. All the RF rectifier designs discussed above use the Schottky diode HSMS-2810 to attain low power levels due to its low forward voltage drop, despite its high series resistance. Figure 26 shows that this rectifying circuit produces a DC voltage of 11.609 V with an efficiency of 8.09% when the incident strength is –20 dBm, and it is roughly 3.1 times more efficient than that of HSMS 8101:

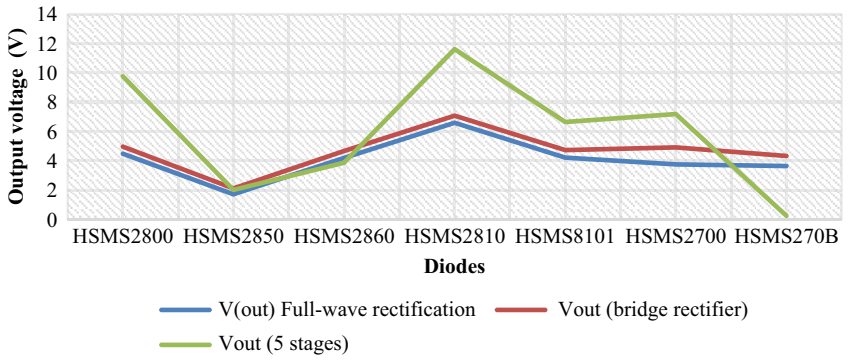

Fig. 26. Comparing the output DC voltages of Schottky diodes: HSMS-2800, HSMS-2850, HSMS-2860, HSMS-2810, HSMS8101, HSMS2700, and HSMS-270B

5 Prototype result and discussion

As shown in Figure 27, we measured the S11 of the fabricated antenna using the Vector Network Analyzer (VNA) TTR506A. We only have S11 = –22.53 dBi, when

the theoretical simulation predicted –28.61. The results indicate that a particle causes the S11 to be lower than the simulation with ADS. Figure 27 shows how the twin inset-feed antenna was matched at 2.45 GHz with significantly reduced reflection.

Fig. 27. Measured return loss, S11

To achieve high performance, all antenna parameters have been analyzed and optimized. The radiation efficiency was 61.11%. The designed patch antenna has a simulated gain of 5.21 dBi, the directivity of 7.22 dBi, the input power (Pin) of 1.343 mW, and the radiated power of 1.349 mW at fr = 2.504 GHz. An analysis of the results indicates that the tested products' values differ from the simulation performed by ADS. These results indicate the benefits of using a twin inset-feed patch antenna for obtaining RF energy. The harvester antenna performed exceptionally well in both the simulated and real measurements. This device can acquire microwave power and convert it to DC energy. According to our simulation, the HSMS 2828 diode provides a suitable output voltage for our solution and scope of work.

RF4 epoxy laminate is used to fabricate a high-gain patch antenna with lower insertion loss, a quieter copper thickness, and lower noise levels. At 2.44 GHz operating frequency, the fabricated high-gain antenna exhibits a gain of 5.25 dBi.

The harvest distance was determined by connecting an RF power supply to the transmitter antenna on the transmitter side and a rectifier to an antenna on the receiver side, as shown in Figure 28.

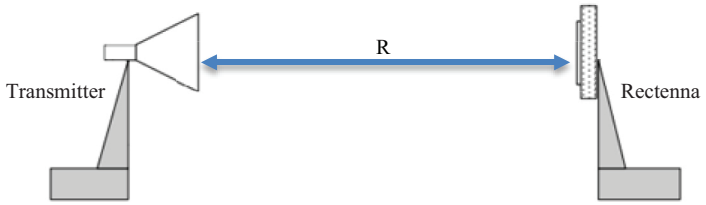

Fig. 28. Block diagram of the transmitter antenna and the integrated rectenna element

Figure 29 shows that the RF transmitted power is 20 W for different distances (1m, 2m, 3m, 4m, and 5m), and the IoT received power is 5 W/12V.

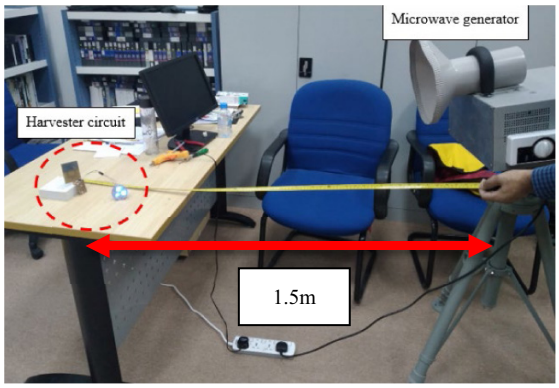

Fig. 29. Photo of RF energy harvesting test setup

The five-stage rectifying circuit was connected to the rectangular patch antenna using a right-angled SMS connector. This device served as a reference in chamber measurements. We successfully powered LED bulbs wirelessly, as shown in Figure 30.

(a) **(b)**

Fig. 30. (a) Photograph of the remote-powering LED bulb 5W, (b) Modified rectifying circuit with a patch antenna

The actual test can show how the efficiency changes due to the distance gap. As shown in Table 8, the quantity of power harvested varies depending on the difference between the microwave power station and the rectenna circuit.

Table 8. Range/distance of energy harvesting

Input RF Power	Gap between the LED Bulb and the RF Generator (R)	Harvested Power
20 W	1 meter	6.63 W
	2 meters	5.34 W
	3 meters	4.81 W
	4 meters	4.02 W
	5 meters	3.31 W

With HSMS-2810 and a patch antenna, the rectenna produces a maximum DC voltage of 11.7 V and an efficiency of 18.75 % at 20W RF power. Figure 31 illustrates how harvesting power varies with the increasing distance gap.

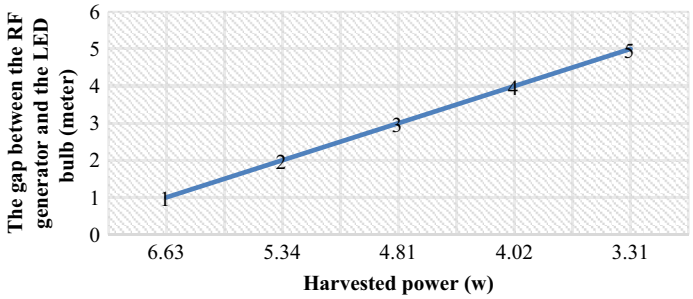

Fig. 31. Energy harvesting range/distance

6 Conclusion and perspectives

In wireless power transmission, radiofrequency energy is transmitted through free space. Power levels are dependent on the location of the IoT sensors the location of the microwave transmitter. IoT network sensors can also be recharged using energy harvesting technology. This device is a wireless battery as opposed to a traditional battery, and it is capable of converting microwave energy from ambient environments into valuable DC energy. We have demonstrated that RF power stations can produce electricity wirelessly. Many electronic devices can be charged inside the smart house through the harvesting circuit or remote powering circuit.

According to a real test, the twin inset-feed antenna achieved a reflection coefficient of –24 dB and a maximum gain direction of 7.33 dB at the S-band. RF harvesting circuits generate high DC output voltages, and ADS was used to simulate rectifying circuits and diode models. Several rectifying circuits are discussed in the RF/DC conversion subsection, including high and low-power rectifying circuits. Using a Schottky diode HSMS2800, a five-stage rectifying circuit with a maximum DC voltage of 9.752 V and a conversion efficiency of 5.91% is achieved with a load resistor of 50Ω when the input power is 33 dB. Another example is the rectifying circuit with Schottky

diodes HSMS-2810. A power level of 33 dB produces a DC voltage of 11.609 V and a conversion efficiency of 8.09%. With an incident power of 33 dBm, and due to energy scavenging at high power densities, the rectifying circuit with Schottky diode HSMS 8101 achieves a DC voltage of 6.641 V and an efficiency of 2.61% over a resistive load 50. With its high efficiency for low power levels, this circuit contributes to the power conversion system from familiar radiation sources. The conversion efficiency was 16.65% at a distance of five meters. Wireless power technology enabled us to energize any electronic device and enhance IoT devices. Smart houses will become more intelligent and reliable due to the use of this technology.

7 References

[1] K. Kawai, N. Shinohara, and T. Mitani, "Design of High Efficiency Rectifier Circuit for 920 MHz Wireless Power Transmission," in *2020 IEEE Wireless Power Transfer Conference (WPTC)*, Seoul, Korea (South), Nov. 2020, pp. 130–133. https://doi.org/10.1109/WPTC48563.2020.9295563

[2] J. Liu, Z. Zhao, J. Ji, and M. Hu, "Research and Application of Wireless Sensor Network Technology in Power Transmission and Distribution System," *Intell. and Converged Netw.*, vol. 1, no. 2, pp. 199–220, Sep. 2020. https://doi.org/10.23919/ICN.2020.0016

[3] Y. Park and D. Youii, "kW-class Wireless Power Transmission Based on Microwave Beam," in *2020 IEEE Wireless Power Transfer Conference (WPTC)*, Seoul, Korea (South), Nov. 2020, pp. 5–8. https://doi.org/10.1109/WPTC48563.2020.9295626

[4] C. Cheng et al., "Load-Independent Wireless Power Transfer System for Multiple Loads Over a Long Distance," *IEEE Trans. Power Electron.*, vol. 34, no. 9, pp. 9279–9288, Sep. 2019. https://doi.org/10.1109/TPEL.2018.2886329

[5] M. Z. Chaari and S. Al-Maadeed, "Increase the Efficiency of IoT Devices by Using the Wireless Power Transmission in the Industrial Revolution 4.0," *Int. J. Onl. Eng.*, vol. 17, no. 07, p. 172, Jul. 2021. https://doi.org/10.3991/ijoe.v17i07.24143

[6] L.-G. Tran, H.-K. Cha, and W.-T. Park, "RF Power Harvesting: A Review on Designing Methodologies and Applications," *Micro and Nano Syst Lett*, vol. 5, no. 1, p. 14, Dec. 2017. https://doi.org/10.1186/s40486-017-0051-0

[7] R. Ren, J. Huang, and H. Sun, "Investigation of Rectenna's Bandwidth for RF Energy Harvesting," in *2020 IEEE MTT-S International Microwave Workshop Series on Advanced Materials and Processes for RF and THz Applications (IMWS-AMP)*, Suzhou, China, Jul. 2020, pp. 1–2. https://doi.org/10.1109/IMWS-AMP49156.2020.9199653

[8] R. K. Sidhu, J. Singh Ubhi, and A. Aggarwal, "A Survey Study of Different RF Energy Sources for RF Energy Harvesting," in *2019 International Conference on Automation, Computational and Technology Management (ICACTM)*, London, United Kingdom, Apr. 2019, pp. 530–533. https://doi.org/10.1109/ICACTM.2019.8776726

[9] C.-Y. Chu et al., "Wireless Power Transfer System Design for Electric Vehicle Charging Considering A Wide Range of Coupling Coefficient Variation Depending on the Coil Misalignment," in *2021 24th International Conference on Electrical Machines and Systems (ICEMS)*, Gyeongju, Korea, Republic of, Oct. 2021, pp. 732–737. https://doi.org/10.23919/ICEMS52562.2021.9634575

[10] K. Ishibashi, J. Ida, L.-T. Nguyen, R. Ishikawa, Y. Satoh, and D.-M. Luong, "RF Characteristics of Rectifier Devices for Ambient RF Energy Harvesting," in *2019 International Symposium on Electronics and Smart Devices (ISESD)*, Badung-Bali, Indonesia, Oct. 2019, pp. 1–4. https://doi.org/10.1109/ISESD.2019.8909660

[11] M. Z. Chaari and R. Al-Rahimi, "The Impact of Wireless Power Charging on the Future of the Battlefield," in *2021 International Wireless Communications and Mobile Computing (IWCMC)*, Harbin City, China, Jun. 2021, pp. 1563–1568. https://doi.org/10.1109/IWCMC51323.2021.9498775

[12] M. Z. Chaari and R. Al-Rahimi, "Energized IoT Devices through RF Wireless Power Transfer," in *2021 International Symposium on Electrical and Electronics Engineering (ISEE)*, Ho Chi Minh, Vietnam, Apr. 2021, pp. 199–203. https://doi.org/10.1109/ISEE51682.2021.9418741

[13] M. Z. Chaari and R. Rahimi, "Light LED Directly Lit Up by the Wireless Power Transfer Technology," in *2017 International Conference on Radar, Antenna, Microwave, Electronics, and Telecommunications (ICRAMET)*, Jakarta, Oct. 2017, pp. 137–141. https://doi.org/10.1109/ICRAMET.2017.8253162

[14] N. A. Eltresy, D. N. Elsheakh, E. A. Abdallah, and H. M. Elhennawy, "Tri-Band Antenna for Energizing IoT Low Power Devices," in *2018 IEEE Global Conference on Internet of Things (GCIoT)*, Alexandria, Egypt, Dec. 2018, pp. 1–5. https://doi.org/10.1109/GCIoT.2018.8620145

[15] D. Pinto et al., "Design and Performance Evaluation of a Wi-Fi Energy Harvester for Energizing Low Power Devices," in *2021 IEEE Region 10 Symposium (TENSYMP)*, Jeju, Korea, Republic of, Aug. 2021, pp. 1–8. https://doi.org/10.1109/TENSYMP52854.2021.9551001

[16] A. J. Casson and E. Rodriguez-Villegas, "Low Power Signal Processing Electronics for Wearable Medical Devices," in *2010 Annual International Conference of the IEEE Engineering in Medicine and Biology*, Buenos Aires, Aug. 2010, pp. 3439–3440. https://doi.org/10.1109/IEMBS.2010.5627856

[17] L. Turicchia et al., "Ultra-Low-Power Electronics for Non-Invasive Medical Monitoring," in *2009 IEEE Custom Integrated Circuits Conference*, San Jose, CA, USA, Sep. 2009, pp. 85–92. https://doi.org/10.1109/CICC.2009.5280892

[18] M. Z. Chaari and S. A. Al-Maadeed, "Spiral Antenna Mounted on the t-Shirt to Harvested RF Energy," in *2019 1st International Conference on Electrical, Control and Instrumentation Engineering (ICECIE)*, Kuala Lumpur, Malaysia, Nov. 2019, pp. 1–6. https://doi.org/10.1109/ICECIE47765.2019.8974756

[19] M. Z. Chaari and S. Al-maadeed, "Wireless Power Transmission for the Internet of Things (IoT)," in *2020 IEEE International Conference on Informatics, IoT, and Enabling Technologies (ICIoT)*, Doha, Qatar, Feb. 2020, pp. 549–554. https://doi.org/10.1109/ICIoT48696.2020.9089547

[20] A. O. Fadamiro et al., "Temperature Variation Effect on a Rectangular Microstrip Patch Antenna," *Int. J. Onl. Eng.*, vol. 15, no. 05, p. 101, Mar. 2019. https://doi.org/10.3991/ijoe.v15i05.9755

[21] Y. Li and Z.-C. Hao, "A Wideband Switched Beam Antenna for Full 360 Coverage," in *2017 Sixth Asia-Pacific Conference on Antennas and Propagation (APCAP)*, Xi'an, Oct. 2017, pp. 1–3. https://doi.org/10.1109/APCAP.2017.8420905

[22] N. Akter, B. Hossain, H. Kabir, A. H. Bhuiyan, M. Yeasmin, and S. Sultana, "Design and Performance Analysis of 10-Stage Voltage Doublers RF Energy Harvesting Circuit for Wireless Sensor Network," *JCEN*, pp. 84–91, Apr. 2014. https://doi.org/10.18005/JCEN0202004

[23] E. M. Ali, N. Z. Yahaya, N. Perumal, M. A. Zakariya, "Development of Cockcroft-Walton Voltage Multiplier for RF Energy Harvesting Applications," *Journal of Scientific Research and Development*, vol. 3, pp. 47–51, 201, 2016.

[24] M. Z. Chaari, R. Rahimi, H. Ghariani, and M. Lahiani, "Microwave Energy Harvesting using Rectangular Micro-Strip Patch Array Antenna," in *2017 Sensors Networks Smart and Emerging Technologies (SENSET)*, Beirut, Sep. 2017, pp. 1–4. https://doi.org/10.1109/SENSET.2017.8125041

8 Authors

Mohamed Zied Chaari, FABLAB Department Doha, Qatar Scientific Club, Doha, Qatar.

Rashid Al-Rahimi, FABLAB Department Doha, Qatar Scientific Club, Doha, Qatar.

Otman Aghzout, Department of Computer Science and Engineering, SIGL-Lab ENSA, Tétouan, Morocco.

Article submitted 2022-03-14. Resubmitted 2022-04-24. Final acceptance 2022-04-24. Final version published as submitted by the authors.